



Journal of Applied and Computational Mechanics



Research Paper

Modeling of the Dynamic Rail Deflection using Elastic Wave Propagation

Dmytro Kurhan¹, Szabolcs Fischer²

¹ Department of Transport Infrastructure, Dnipro National University of Railway Transport named after Academician V. Lazaryan, Lazaryan st. 2, Dnipro, 49010, Ukraine, Email: kurhan.d@diit.edu.ua

² Department of Transport Infrastructure and Water Resources Engineering, Széchenyi István University, Egyetem tér 1, Győr, 9026, Hungary, Email: fischersz@sze.hu

Received October 11 2021; Revised November 16 2021; Accepted for publication November 26 2021.

Corresponding author: S. Fischer (fischersz@sze.hu)

© 2022 Published by Shahid Chamran University of Ahvaz

Abstract. There is a class of tasks that requires considering the dynamics not only for rolling stock but also for the response of the railway track. One of the directions of railway transport development, which encourages the transition to fundamentally new dynamic models of the railway track, is undoubtedly an increase in traffic speed. To solve such problems, the authors applied a model of the stressed-strained state of a railway track based on the dynamic problem of elasticity theory. The feature of this model is the calculation of dynamic stresses and deformations induced by the spread of elastic waves through the objects of the railway track. Based on the mathematical modeling of stress propagation in the under-rail basis, authors have shown the influence of various objects of a railway track on the formation of the outline of the front of the elastic wave and determined the main time intervals. Furthermore, the authors propose the following analytical method, which, in addition to the soil's physical and mechanical properties, considers the properties of the ballast as a layer that transmits pressure to the roadbed and takes an active part in the formation of the interaction space.

Keywords: Railway, ballast, stressed-strained state, dynamic stress, elastic wave.

1. Introduction

Several variants of the mathematical notation of a railway track are used in many problems related to the interaction between a track and the rolling stock. First of all, they can be divided into static, quasi-static, and dynamic models. For static and quasi-static models, the main characteristic of the track is its rigidity in one or another manifestation. Depending on the problem being solved and following the mathematical model applied, different detailed descriptions of the railway track are possible. Starting from the beam (i.e., the rail), which rests on a uniformly elastic base, to determining individual supports (i.e., the sleepers), followed (if necessary) by the distribution of the ballast layer into conditional objects that interact with a separate sleeper, which necessitates taking into consideration not only vertical connections but also horizontal and longitudinal ones. The densest breakdown of a railway track into individual objects is typically employed by FEM-based models, which is one of the fundamental requirements for applying this approach.

For a long time, the stressed-strained state of the railway track was described by static models, or quasi-static, which in one form or another took into consideration the dynamics of workload on the track. That required the use of a series of hypotheses and assumptions while significantly reducing the volume of computations. For many tasks, that approach can be considered adequate today. However, there is a class of tasks that requires taking into consideration the dynamics not only for rolling stock but also for the response of the railway track. One of the directions of railway transport development, which encourages the transition to fundamentally new dynamic models of the railway track, is undoubtedly an increase in the speed of traffic [1–3], including sections of international transport corridors [4, 5].

While the static and quasi-static models are limited to considering rigid connections between objects, the dynamic models can be supplemented with dissipative links and, in some cases, masses. Thus, each object is in a dynamic equilibrium, which is described by the differential equation of the second power, taking into account the force through the product of the object's mass at its acceleration, which is balanced by the connections of rigidity and dissipation with adjacent objects. Today, this approach is the most common for constructing mathematical models of rolling stock carriages [6–9], which can be relatively easily divided into separate completely rigid (without deformation of the form) objects with a mass concentrated at a point. Given the requirement for the uniform assignment of all the objects that make up a mathematical model, the same approach is used for railway track elements.



Dividing of the railway track into such separate objects causes specific difficulties and conditions. The railway track is more consistent with the layered semi-space, which works on elastic deformations, than a set of connected elements that work to move (change the position of the center of their masses). At present, however, there are adequate solutions to such a problem. They are associated with a compromise between sufficient but not unnecessary detailing of the railway track into individual objects and the use of a conditional (adjusted) mass as a characteristic whose presence is a forced property of a given mathematical approach.

Naturally, such characteristics as dissipation and mass (adjusted mass) translate the model to a dynamic class. However, regarding the railway track, additional explanations are needed about what kind of dynamic work is in question.

First, the railway track consists of a certain number of elements under such representation, which immediately limits its actual length in space. Then, typically, the part of the track that is in contact with the wheel (or with the bogie/vehicle, as a wheel system) is introduced into the model, which allows the simulation of its deflection and, inversely, provides for appropriate reactions from the track to the rolling stock. The length of the railway track and the depth of the under-rail base are sufficient for implementing the "complete" deflection, depending on a series of factors, but the problem of their consideration may have a solution.

Second, with this approach, all the elements into which the section of the track is divided for introduction into the model interact simultaneously. Due to the elements' dissipated connections and mass (an indicator of inertia), there will be some delay in moving objects to places corresponding to the formation of complete deflection of the track; however, all objects of the system are involved in the process of interaction at once.

The railway track is better described as a layered system of bodies working on elastic deformations. In any body, stresses (and, accordingly, strains) have a finite velocity of propagation, which depends on such physical properties as density (ρ), Young modulus (E), and Poisson's ratio (μ). In general, there is a longitudinal velocity of propagation (C_1), which coincides with the direction of the applied force, and transverse (C_2), which is perpendicular to the direction of the force application

$$C_1 = \sqrt{\frac{E(1-\mu)}{\rho(1+\mu)(1-2\mu)}} \quad (1)$$

$$C_2 = \sqrt{\frac{E}{2\rho(1+\mu)}} \quad (2)$$

The rate of stress propagation in any direction α , where $\alpha = 0^\circ$ corresponds to the longitudinal direction, i.e. matches the direction of force ($C_\alpha = C_1|\alpha = 0$) and $\alpha = 90^\circ$ transverse ($C_\alpha = C_2|\alpha = 90^\circ$), is then can be determined from the following equation given in [10]

$$C_\alpha = \frac{C_1 C_2}{\sqrt{C_1^2 \sin^2 \alpha + C_2^2 \cos^2 \alpha}} \quad (3)$$

It should be noted that the railway track has such a structure that its rigidity decreases in the direction of external load; that is, its stiffer layers (rails, sleepers) enter the interaction first, followed by its softer layers (ballast, supplementary layer, soil). In terms of elasticity theory, the position of the rigid layer on a softer one is a more complex case than vice versa. This arrangement of layers in terms of rigidity leads to the lower layers' strain propagation rate being less. The contact zone between the layers (a pressure transfer zone from the upper, more rigid, to the lower, softer) then increases faster than the wave propagation in the next layer. One factor significantly complicates the calculations of the geometry of the spread of stress waves in the railway track and makes it impossible to reduce them to basic Eqs. (1–3).

2. The Current State of the Problem

The issue, related to the need to consider the dynamics of a railway track response when a train runs, is long overdue. It acquired special relevance and practical significance when high-speed and ultra-high-speed trains became common. Below are examples of some recently written papers whose authors address the issue of the need to move from a static deflection of the track, which occurs instantly, to a dynamic process unfolding over time.

The current state of mathematical modeling aimed at studying the work of a railway track under conditions of high speeds of movement was analyzed in papers [11, 12] and others.

Paper [13] describes the problem of the impossibility of increasing the speed of traffic along the sections of a railway track with weak soils. One of the reasons for this situation is the appearance of dynamic effects in the space of a railway track when approaching critical speed due to the characteristics of soil deformation.

Papers [14, 15] show a change in the stressed-strained state of a railway track at high speeds due to the tangible amplitude of the propagation of waves in the soil. In the cited work [15], the hypothesis of dependence on the amplitude and the depth of the spread of such waves on the train's speed is put forward.

Options for considering the dynamic response of the under-rail basis in the mathematical model of track and rolling stock interaction are proposed in [16].

Vibration effects were registered and investigated along the high-speed railway sections in China. Paper [17] reports the relevant experimental and theoretical results using an example of the Beijing-Zhangjiakou section.

Studies [18, 19] prove a "critical speed problem" at the speeds of trains approaching the speed of waves spreading within the space of a railway track. Several papers [20–22] have proposed measures to reduce vibrations induced by the propagation of waves in the soil during such phenomena.

Paper [23] considers the formation and evolution of voids in ballast under sleepers. The basis for the mathematical methods that have been applied is the dynamic interaction between the elements of the railway track, namely the elastic movement of sleepers with a certain acceleration during the deflection of the rail.

The development of considering the stressed-strained state of a railway track due to the spread of elastic waves within its space led to the emergence of new methods for examining the state of the track. Thus, papers [24, 25] proposes a method for assessing the state of ballast according to the results of measuring the passage of waves through the space of the under-rail base; paper [26, 27] – for evaluating the state of a roadbed.

The need to consider the dynamic properties of the under-rail base is characteristic not only of main railways but also of the subway [28]. Thus, papers [29, 30] tackle the problems of the distribution of vibrations along the sections of subways.



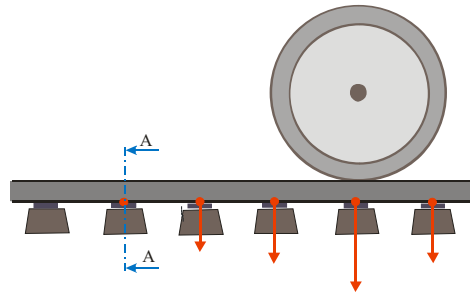


Fig. 1. Change in the pressure forces from the rail to supports as a representation of wheel movement.

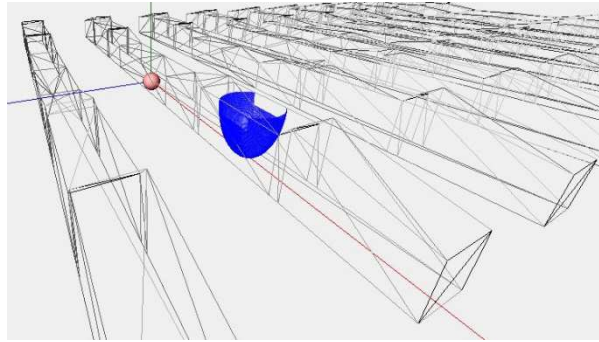


Fig. 2. Stress propagation front in a sleeper at the time of the start of the pressure on the ballast.

3. A Method for the Mathematical Modeling of Dynamic Rail Deflection

3.1 General provisions

To solve such problems, the authors applied a model of the stressed-strained state of a railway track based on the dynamic problem of elasticity theory, the basic provisions of which are given in paper [10]. The feature of this model is the calculation of dynamic stresses and deformations induced by the spread of elastic waves through the objects of the railway track. The sites of application of external load are used to construct a set of vectors in all directions of the semi-space. The length of a separate vector depends on the time step and the rate of wave propagation in a given direction, which, in turn, is determined concerning the longitudinal and transverse velocity of elastic waves propagation in a substance through which a given vector passes. Then the surface formed by the ends of the vectors is the front of elastic wave propagation and, accordingly, of the stresses and strains within a given time step of calculations.

The spread of stresses along the length of a rail is not the same as the formation of its deflection. Deflection of the rail is formed by deformation of all layers of the under-rail base. For complete deflection of the rail, the corresponding deformations must be implemented within the space of the under-rail base of a certain depth and length.

Pressure from one wheel due to the deflection of the rail is transmitted not only to the central sleeper (one that is directly in the cross-section of the wheel location) but also to several adjacent sleepers. The deflection length depends on the rigid characteristics of the rail and the under-rail base, and the deflection amplitude also depends on the size of the wheel load on the rail. The "tangible" impact extends to 2-3 sleepers relative to the central one [11]. Changing the wheel's position along the length of the rail does not directly change the coordinates of applying forces to the under-rail base but redistributes pressure to fixed supports. Over the time of the wheel movement, the system will be "supplemented" with the new loads on the support, and, accordingly, the unloaded ones will be "removed" (Fig. 1).

3.2 Stress propagation induced by an instantaneously applied single force

Authors accept that the estimation region at the time $t=0$ is exposed to the action of force corresponding to the cross-section "A-A" in Fig. 1. In the beginning, consider the process of the evolution and propagation of stresses in a railway track induced by the action of such a single external load. This will allow to analyze the general provisions of stress propagation. Subsequently, the results to be obtained could be expanded by considering the forces from adjacent sleepers. The value of force (or, more precisely, the growth of its value in the process of approaching the wheel to the estimated cross-section) is also not required at this stage, given that the speed and geometry of the spread of stresses do not depend on the level of force.

First, the pressure from the rolling stock wheel is transferred to the rail. The rate of strain propagation in a metal rail is very high, and, for example, for the UIC60 rails, it is 5,856 m/s in the longitudinal direction and 3,130 m/s in the transverse direction, respectively. Thus, the pressure from the rail would reach the central sleeper in $3 \cdot 10^{-5}$ s, and, in $17 \cdot 10^{-5}$ s, would reach the first adjacent sleeper. After this, time marks are given relative to the moment of conditionally sudden application of force to the estimated cross-section.

Inside the body of a reinforced concrete sleeper, stresses spread slower than in the rail, but still very quickly: 4,736 m/s longitudinal and 2,532 m/s transverse velocity, respectively. Fig. 2 shows the front of stress propagation within the space of a reinforced concrete sleeper in $5 \cdot 10^{-5}$ s.

Mathematical modeling of the process of stress propagation was carried out for the complete structure of the track, which consisted of rails, rail fasteners, sleepers, ballast, and soil roadbed. However, to improve the visual perception, Fig. 2 and subsequent drawings demonstrate only the contours of sleepers of all the railway track elements. At this time mark, the front of stress propagation takes an almost ellipsoidal shape, but is corrected by the outlines of the sleeper and the surface of the load application.



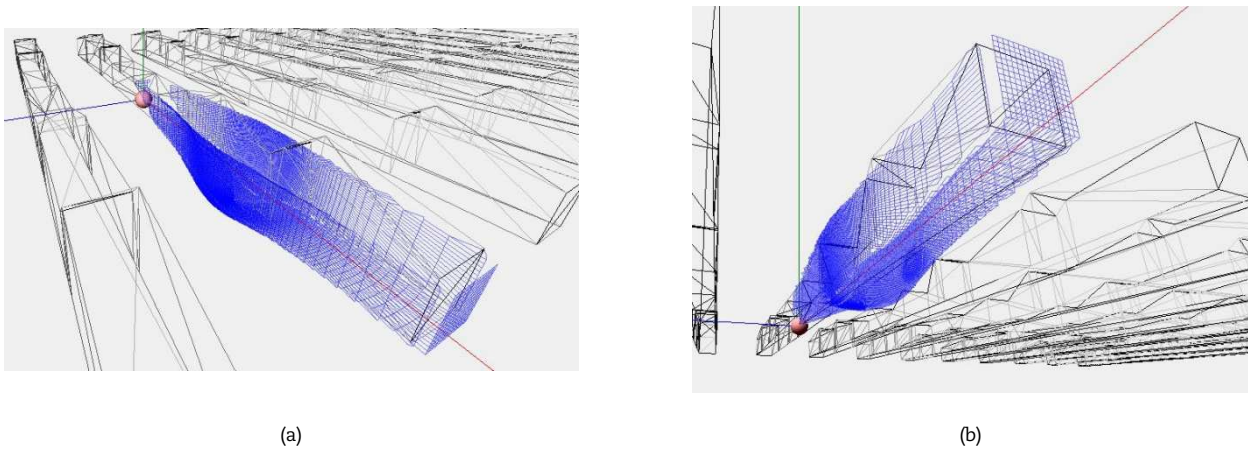


Fig. 3. The front of stress propagation has reached the middle of the sleeper: a) – top view; b) – bottom view.

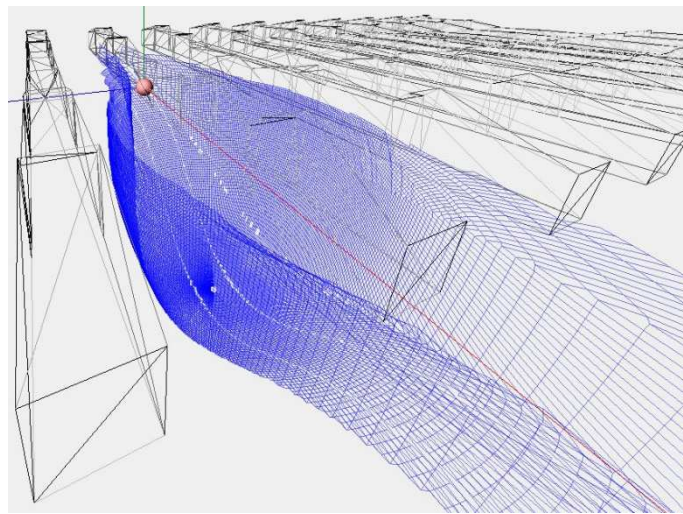


Fig. 4. The front of stress propagation at the time of the beginning of pressure on the roadbed.

Further, ballast is involved in the interaction process. The propagation of stresses in the ballast would occur much slower than in the reinforced concrete sleeper. Therefore, the outline of the propagation at the surface of the ballast (the contact zone between the sleeper and ballast) would be formed for some time due to the spread of stresses in the sole of the sleeper. At the time mark of $23 \cdot 10^{-5}$ s from the onset of force application, the front of stress propagation in a sleeper would reach its edge, and, at the mark of $23 \cdot 10^{-5}$ s, the middle of the sleeper (Fig. 3). Starting from this moment, the process of forming the outline of the pressure transfer surface from the sleeper to the ballast can be considered complete. Fig. 3 (part b) shows this surface with the beginning of deepening into the ballast layer. Further propagation of the front of stresses in the ballast would occur due to its properties. Some additional adjustments to the outline of the front would be made when adjacent sleepers are involved in the process.

A ballast layer can have different geometric dimensions, different materials with different physical and mechanical properties, enter a different state of compaction and pollution, etc. All of them have a significant impact on its stressed-strained state [31, 32], including the rate of stress propagation. In the estimation variant, the example of which is considered in the current work, gravel ballast with a thickness of 0.6 m with a deformation module of 200 MPa has been adopted. With such initial characteristics, the rate of stress propagation in the ballast would equal 410 m/s in the longitudinal direction and 219 m/s in the transverse directions, respectively. In this case, the transfer of pressure from ballast to the roadbed would begin at $151 \cdot 10^{-5}$ s. The corresponding outline of the stress propagation front within the space of a railway track is shown in Fig. 4. It should be noted that at this moment, the spread of stresses on the surface of the ballast does not yet have time to reach adjacent sleepers.

The rate of stress propagation in a soil bed (soil layer), as in the case of a ballast layer, can vary in a certain range, depending on the soil's physical and mechanical properties that make up the roadbed. In a given example, the soil with a deformation modulus of 35 MPa was accepted. The stress propagation rates, in this case, were 183 m/s in the longitudinal direction and 98 m/s in the transverse direction, respectively. The outline of the propagation front will be corrected by the faster spread of stresses on the contact surface of the ballast and soil bed compared to the propagation rates in the soil, and, subsequently, the emergence of additional pressure on ballast from adjacent sleepers. This shape of the outline of stress propagation in a railway track for $423 \cdot 10^{-5}$ s, which, for the above initial data, corresponds to the depth of propagation in the soil along the axis of force action by 0.5 m, is shown in Fig. 5.

To simplify the visual perception and analysis of the results, the further formation of the outline of the space of the railway track, which has already entered the interaction process, is shown in a flat form along the cross-section of the longitudinal axis of the rail, Fig. 6. Fig. 6 horizontally shows the distance from the estimated cross-section (Fig. 1), vertically – the depth relative to the sole of the sleeper. Explanations of the modeling results numbered in this plot are summarized in Table 1.



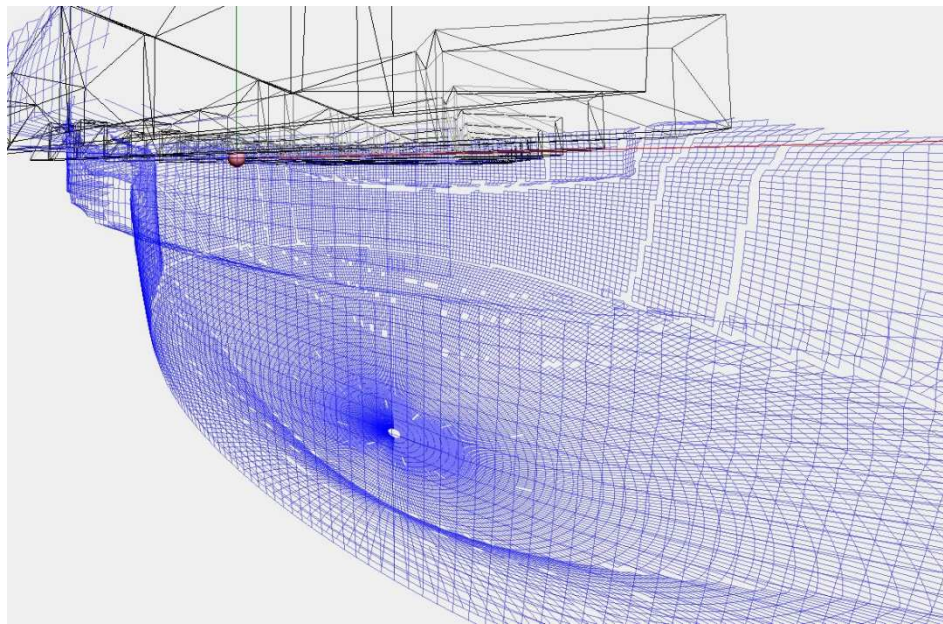


Fig. 5. The front of stress propagation in the space of a railway track reaches the soil depth of 0.5 m.

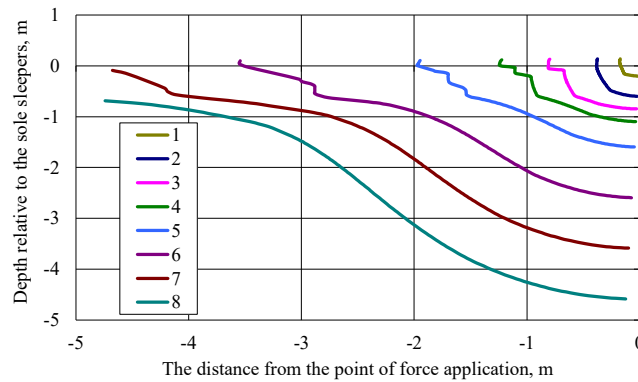


Fig. 6. The front of stress propagation in the space of a railway track along the rail.

During the described modeling of stress propagation within the space of a railway track, authors calculated the elastic deformations of the under-rail base [10] and analyzed their sufficiency for the implementation of the complete deflection of the rail. A known equation for the static deflection of the rail as a beam resting on an equally elastic base was taken as a basis

$$z = \frac{Pk}{2U} e^{-kx} (\cos kx + \sin kx), \tag{4}$$

where z – is the deflection of the rail; P – is the force acting from the wheel to the rail; U – is the module of elasticity of the under-rail base; x – is the distance from the point of force application to the point of deflection calculation; k – is the relative rigidity coefficient

$$k = \sqrt[4]{\frac{U}{4EI}}, \tag{5}$$

where E - is the rail steel elasticity modulus; I - is the moment of inertia of the rail.

Table 1. Description of the estimated positions shown in Fig. 6

Line number in Fig. 6	Time mark, s	Vertical mark long the axis of force application	3D image
1	54 · 10 ⁻⁵	ballast, 20 cm	
2	151 · 10 ⁻⁵	ballast, 60 cm, roadbed surface	Fig. 5
3	287 · 10 ⁻⁵	roadbed, 0.25 m	
4	423 · 10 ⁻⁵	roadbed, 0.5 m	Fig. 6
5	695 · 10 ⁻⁵	roadbed, 1.0 m	
6	1,239 · 10 ⁻⁵	roadbed, 2.0 m	
7	1,783 · 10 ⁻⁵	roadbed, 3.0 m	
8	2,327 · 10 ⁻⁵	roadbed, 4.0 m	



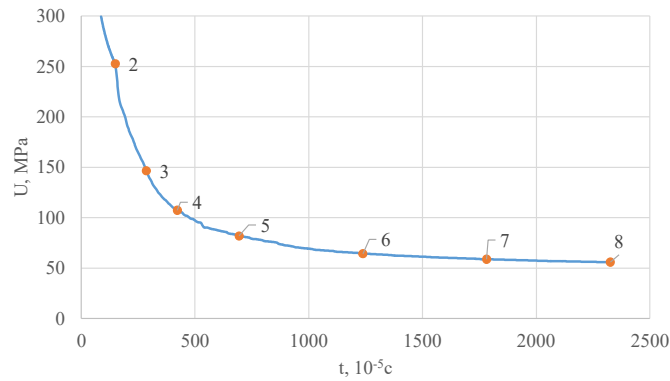


Fig. 7. Change in the overall rigidity of the under-rail base over the time of stress propagation (explanations for the number of points are provided in Table 1).

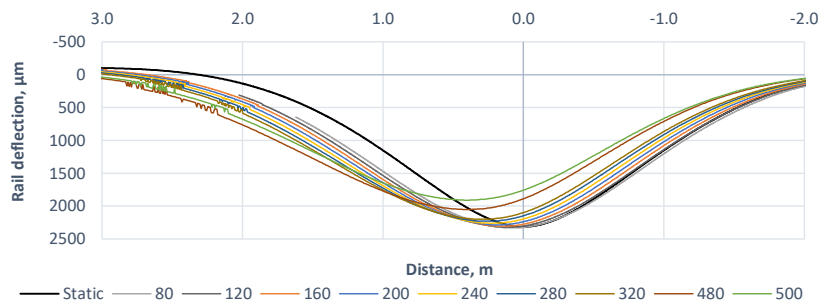


Fig. 8. Dynamic deflections of the rail depending on the speed of movement for the section with $U = 32$ MPa.

Based on the values of the dynamic deflection of the rail along its length ($\{z_x^*\}$), derived from the results of modeling, authors determined the module of elasticity of the under-rail base identical to the implementation of the deflection of the same shape, but static

$$\exists U: \sum_x (z_x - z_x^*)^2 \rightarrow \min. \tag{6}$$

Fitting the derived value of the under-rail base elasticity module to the asymptote shows the implementation of the complete deflection of the rail. Fig. 7 demonstrates a plot of change in this indicator within the framework of the numerical example under consideration. Separate points illustrate the estimated variants corresponding to Fig. 6 and Table 1.

Based on Fig. 7 and Table 1, authors can argue regarding this demonstration example that when an elastic wave spreads to a depth of about 3.0 m, an under-rail base space is formed, including the length of the section, sufficient to form a deflection of the rail identical to static.

3.3 Modeling the dynamic rail deflection induced by a moving load

Let us consider how the rail deflection will change in the experimental cross-section during the passage of the wheel from a distance when the pressure is not yet present to a distance when the pressure is no longer present. The resulting outline of the deflection of the rail will be termed dynamic, bearing in mind that it was obtained considering the dynamics of deflection of the under-rail base. For comparison, the outline of the deflection obtained according to the known equations of static deflection of the rail as a beam on an equally elastic basis induced by the load identical to dynamic, will be termed static.

Differences in the dynamic and static deflection are more indicative when moving at high speeds and for structures with low stiffness. For the above numerical example, the under-rail base elasticity modulus is 56 MPa (Fig. 7). For clarity, authors shall consider further the "softer" structure of a railway track: rails, UIC60; reinforced concrete sleepers; gravel ballast (deformation modulus, 200 MPa), 0.5 m thick from the sole of the sleeper; soil with a deformation module of 25 MPa. The accepted data correspond to the calculation-based (Eq. (6)), similar to those shown in Fig. 7, total elasticity module of the under-rail base at the level of 32 MPa. Calculations were performed for speeds from 80 to 320 km/h, including increments of 40 km/h, due to a moving force of 145 kN. The calculation results are shown in Fig. 8. For comparison, the figure also demonstrates the outline of a static deflection of the rail, calculated from Eq. (4).

The authors' analysis of the calculation results, the example of which is shown in Fig. 8, reveals that with increased speed of movement, there is a change in the outline of the deflection of the rail, which is a consequence of the manifestation of the dissipative properties of the layers of the under-rail base. However, these changes are small, and characteristics such as the maximum deflection value and its length remain almost constant. Therefore, the stresses that arise in the under-rail base during this process may differ in the speeds of implementation but, in terms of the maximum values, are identical to the quasi-static ones. Figure 8 additionally shows the outlines of rail deflection for speeds of 480 and 500 km/h. It is an example of speeds at which such a track design will no longer have time to implement the "complete" deflection of the rail.

The established differences in the reaction of the rail between dynamic and static deflection are the basis for the justified determination of such characteristics as dissipation and the adjusted weight of elements of the railway track required for a series of mathematical models of interaction between a track and the rolling stock [33].



3.4 Determining the outline of the front of interaction in the under-rail base analytically

One of the basic principles that make it possible to simulate the stressed-strained state of a railway track with spatial-temporal consideration of the dynamics of deflection of the under-rail base is to determine and take into account the outline of the space participating in the interaction at a given time mark of calculation. In addition to the tasks of determining the dynamic indicators of stresses or deformations that require accurate step-by-step determination of the spatial outline of the front surface, there are other areas of calculation for which it would suffice to determine the general characteristics of propagation or a degree of propagation at the time of meeting the specified boundary conditions, etc. These are the tasks of justifying the place of installation (or other characteristics) of protective layers (or structures), the size of the estimated space when simulating a railway track, for example, by a finite element method, etc. In this case, one needs to analytically calculate the outline of the interaction space according to certain conditions.

For a single-layer structure, which, in terms of size, can be considered a semi-space, the solution to such a problem in polar coordinates is derived from Eq. (3)

$$r(\alpha, t) = C_{\alpha}t. \tag{7}$$

In other words, having the physical characteristics of the layer, namely the deformation module, density, Poisson coefficient, one can determine the length of the radius vector ($r(\alpha, t)$) from the point of force application at the time of calculation in the desired direction α . The geometric outline obtained as a result would take the form of an ellipse (an oval for a flat problem).

This approach (with a certain error) may be acceptable for the ballast layer. The elements of the upper structure of the track located above it change the shape of the propagation front. Still, given the high speed of passing spatial waves in them, in comparison with the ballast, this error can be considered acceptable for most problems.

The outline of the propagation front in a soil bed accepts a more complex shape (Figs. 5 and 6). To determine it by the analytical method, authors propose the following equation, which, in addition to the physical and mechanical properties of the soil, takes into consideration the properties of the ballast as a layer that transmits pressure to the roadbed and takes an active part in the formation of the interaction space

$$r(\alpha, t) = \frac{\varphi_{(s)}C_{1(s)}t}{\sqrt{\varphi_{(s)}^2\cos^2\alpha + \sin^2\alpha}} + \frac{h_{(b)}}{\cos\alpha} \left(1 - \sqrt{\frac{E_{(s)}\rho_{(b)}}{E_{(b)}\rho_{(s)}}} \right), \tag{8}$$

where $C_{1(s)}$ – is the longitudinal rate of wave propagation in a soil bed, Eq. (1); $h_{(b)}$ – is the thickness of the ballast layer; $E_{(b)}$, $E_{(s)}$ – are the ballast and soil deformation module, respectively; $\rho_{(b)}$, $\rho_{(s)}$ – are the density of a ballast and soil substance, respectively $\varphi_{(s)}$ – is the ratio of transverse velocity to longitudinal for soil

$$\varphi = \sqrt{\frac{1-2\mu}{2(1-\mu)}}. \tag{9}$$

The parameter φ is determined only by the Poisson coefficient. For most bulk substances, it can be accepted that its value is 0.3. Eq (8) can then be simplified

$$r(\alpha, t) = \frac{0.62t\sqrt{E_{(s)}}}{\sqrt{\rho_{(s)}(1-0.71\cos^2\alpha)}} + \frac{h_{(b)}}{\cos\alpha} \left(1 - \sqrt{\frac{E_{(s)}\rho_{(b)}}{E_{(b)}\rho_{(s)}}} \right), \tag{10}$$

If necessary, the result can be reproduced in the Cartesian coordinate system

$$\left. \begin{aligned} x &= r\sin\alpha; \\ z &= r\cos\alpha \end{aligned} \right\}. \tag{11}$$

In the obtained equations, it is accepted that the level $z = 0$ corresponds to the sole of the sleeper, and the time mark $t = 0$ corresponds to the onset of force action.

To compare the outline of the space of stress propagation in a soil bed for estimation options 5–8 (see Fig. 6), calculations were performed following Eq. 10 and Fig. 9. The initial data had the following values: the thickness of the ballast layer, 0.6 m; ballast deformation modulus, 200 MPa; soil, 35 MPa; ballast density, 1,600 kg/m³; soil, 1,400 kg/m³. Calculations in line with the analytical equation have some differences in comparison with the results of modeling, which is explained by a limited list of factors, which is taken into consideration in Eq. 10, and certain simplifications of process physics. However, they convey the general outline of the front of stress propagation both qualitatively and numerically, so this approach can be applied in a series of problems as a component for other mathematical methods and models.

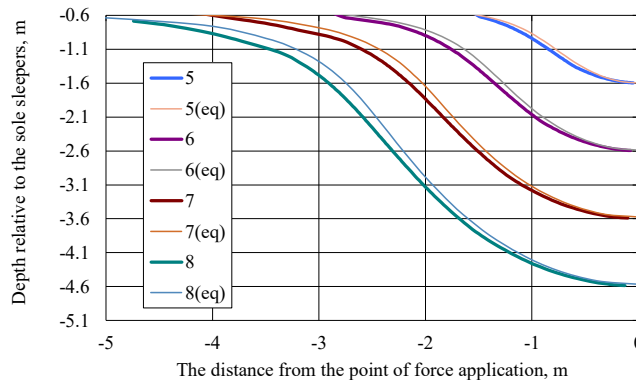


Fig. 9. Comparing the outline of the front of stress propagation in the soil, obtained according to the modeling results and from Eq. (10): line numbers correspond to Table 1.



4. Conclusion

Considering the dynamics of inflection of the railway track is a relevant element of modern mathematical models of interaction between a track and the rolling stock, especially for high speeds of movement. The process of formation of stresses and deformations in the space of a railway line corresponds to the propagation of elastic waves. Therefore, to form a deflection of the rail, the interaction process should include a certain space of the under-rail base, whose elastic deformations, both in depth and in the length of the rail, would ensure its deflection. Therefore, to model the front of stress propagation, the railway track should be considered as a complex multilayer system consisting of sections with different wave propagation rates.

Based on the mathematical modeling of stress propagation in the under-rail basis, authors have shown the influence of various objects of a railway track on the formation of the outline of the front of the elastic wave and determined the main time intervals. It is shown that with an increase in the speed of movement, there is a change in the outline of the deflection of the rail, which is a consequence of the manifestation of the dissipative properties of the layers of the under-rail base. This is the basis for obtaining numerical values of dissipative and inertial characteristics of the railway line, necessary for a series of mathematical models. Upon reaching sufficiently high speeds of movement, the complete deflection may not have time to be implemented. Moreover, the appearance of such effects is determined by the speed of involving the interaction of space both in depth and in the length of the section.

The outline of the front of stress propagation in a specific place within the railway space depends not only on the physical and mechanical properties of this substance but also on the outline of the pressure transfer from the preceding layers. The influence of the upper layers is especially noticeable for the soil. For ballast, it is also true, but the sleeper (as an object that transfers pressure to ballast) has a small area of contact with the ballast compared to the overall surface of the ballast prism, and the influence of adjacent sleepers quickly disappears. For a roadbed, the influence of the top layer is constant due to the length of contact with the ballast. Authors propose the following analytical method, which, in addition to the soil's physical and mechanical properties, considers the properties of the ballast as a layer that transmits pressure to the roadbed and takes an active part in the formation of the interaction space.

Author Contributions

All authors made a substantial, direct, and intellectual contribution to this work. The manuscript was written through the contribution of all authors. All authors discussed the results, reviewed and approved the final version of the manuscript.

Acknowledgments

Not applicable.

Conflict of Interest

The authors declared no potential conflicts of interest concerning the research, authorship, and publication of this article.

Funding

The authors received no financial support for the research, authorship, and publication of this article.

Data Availability Statements

The datasets generated and/or analyzed during the current study are available from the corresponding author on reasonable request.

References


- [1] Hubar, O., Markul, R., Tiutkin, O., Andrieiev, V., Arbusov, M., Kovalchuk, O. Study of the interaction of the railway track and the rolling stock under conditions of accelerated movement, *IOP Conf. Ser.: Mater. Sci. Eng.*, 985, 2020, 012007.
- [2] Zhang, J., Zhang, J. Comprehensive Evaluation of Operating Speeds for High-Speed Railway: A Case Study of China High-Speed Railway, *Mathematical Problems in Engineering*, 1, 2021, 1-16.
- [3] Rashidi, M.M., Hajipour, A., Li, T., Yang, Z., Li, Q. A review of recent studies on simulations for flow around high-speed trains, *Journal of Applied and Computational Mechanics*, 5(2), 2019, 311-333.
- [4] Kurhan, M., Kurhan, D. The effectiveness evaluation of international railway transportation in the direction of 'Ukraine - European Union', *Transport Means 2018, Proceedings of the 22nd International Scientific Conference*, Trakai, Lithuania, 2018.
- [5] Horvat, F., Fischer, S. Magistrale für Europa. *Közlekedésépítési Szemle*, 59 (5), 2009, 33-37.
- [6] Sharma, S.K., Sharma, R.C., Palli, S. Rail vehicle modeling and simulation using lagrangian method, *International Journal of Vehicle Structures and Systems*, 10(3), 2018, 188-194.
- [7] Shvets, A.O. Dynamic Indicators Influencing Design Solution for Modernization of the Freight Rolling Stock, *FME Transactions*, 49(3), 2021, 673-683.
- [8] Shvets, A. Influence of lateral displacement of bogies on the freight car dynamics, *Science and Transport Progress*, 5(89), 2020, 142-159.
- [9] Fomin, O., Gerlici, J., Vatulia, G., Lovska, A., Kravchenko, K. Determination of the Loading of a Flat Rack Container during Operating Modes, *Applied Sciences*, 11(16), 2021, 7623.
- [10] Kurhan, D., Kurhan, M. Modeling the Dynamic Response of Railway Track, *IOP Conference Series: Materials Science and Engineering*, 708, 2019, 012013.
- [11] Kurhan, D. Determination of Load for Quasi-static Calculations of Railway Track Stress-strain State, *Acta Technica Jaurinensis*, 9(1), 2016, 83-96.
- [12] Connolly, D.P., Dong, K., Costa, P.A., Soares, P., Woodward, P.K. High speed railway ground dynamics: a multi-model analysis, *International Journal of Rail Transportation* 8(4), 2020, 324-346.
- [13] Ruiz, J.F., Miranda, M., Castro, J., Rodríguez, L.M. Improvement of the critical speed in high-speed ballasted railway tracks with stone columns: A numerical study on critical length, *Transportation Geotechnics*, 30(4), 2021, 100628.
- [14] Kece, E., Reikalas, V., De Bold, R., Ho, C.L., Robertson, I., Forde, M.C. Evaluating ground vibrations induced by high-speed trains, *Transportation Geotechnics*, 20, 2019, 100236.
- [15] Khan, R., Dasaka, S.M. Spatial Variation of Ground Vibrations in Ballasted High-Speed Railway Embankments, *Transportation Infrastructure Geotechnology*, 7(2), 2020, 354-377.
- [16] Li, T., Su, Q., Kaewunruen, S. Saturated Ground Vibration Analysis Based on a Three-Dimensional Coupled Train-Track-Soil Interaction Model, *Applied Sciences*, 9(23), 2019, 4991.
- [17] Luoa, Q., Fub, H., Liua, K., Wanga, T., Feng, G. Monitoring of train-induced responses at asphalt support layer of a high-speed ballasted track, *Construction and Building Materials*, 298, 2021, 123909.
- [18] Chumyten, P., Connolly, D., Dong, K., Costa, P., Soares, P., Woodward, P. The use of multiple models to analyse railway track ground dynamics,




EURODYN 2020, Athens, Greece, 2020.

- [19] Colaço, A., Alves Costa, P. Geotechnical challenges in very high speed railway tracks. The numerical modelling of critical speed issues, *Construct- FEUP*, Porto, Portugal, 2018.
- [20] Khan, R., Dasaka, S.M. EPS Geofom as a Wave Barrier for Attenuating High-Speed Train-Induced Ground Vibrations: A Single-Wheel Analysis, *International Journal of Geosynthetics and Ground Engineering*, 6(4), 2020, 1-3.
- [21] Denise-Penelope, N., Kontoni, A.A.F. Mitigation of train-induced vibrations on nearby high-rise buildings by open or geofom-filled trenches, *Journal of Vibroengineering*, 22(2), 2020, 416-426.
- [22] Farghaly, A.A. Seismic analysis of adjacent buildings subjected to double pounding considering soil-structure interaction, *International Journal of Advanced Structural Engineering*, 9(1), 2017, 1-12.
- [23] Sysyn, M., Przybylowicz, M., Nabochenko, O., Liu, J. Mechanism of Sleeper-Ballast Dynamic Impact and Residual Settlements Accumulation in Zones with Unsupported Sleepers, *Sustainability*, 13, 2021, 7740.
- [24] De Bold, R., Connolly, D.P., Patience, S., Lim, M., Forde, M.C. Using impulse response testing to examine ballast fouling of a railway tracked, *Construction and Building Materials*, 274, 2021, 121888.
- [25] Sysyn, M., Gerber, U., Nabochenko, O., Kovalchuk, V. Common crossing fault prediction with track based inertial measurements: statistical vs. mechanical approach, *Pollack Periodica*, 14, 2019, 15-26.
- [26] Sysyn, M., Kovalchuk, V., Gerber, U., Nabochenko, O., Parneta, B. Laboratory evaluation of railway ballast consolidation by the non-destructive testing, *Communications - Scientific Letters of the University of Zilina*, 2019, 21(2), 81-88.
- [27] Sysyn, M., Nabochenko, O., Kovalchuk, V., Gerber, U. Evaluation of railway ballast layer consolidation after maintenance works, *Acta Polytechnica*, 59(1), 2019, 77-87.
- [28] Boiko, V., Molchanov, V., Tverdomed, V., Oliinyk, O. Analysis of Vertical Irregularities and Dynamic Forces on the Switch Frogs of the Underground Railway, *MATEC Web of Conferences*, 230, 2018, 01001.
- [29] Wang, L., Bu, X., Han, Y., Zhu, Z., Hu, P., Cai. C.S. Time-Frequency Random Approach for Prediction of Subway Train-Induced Tunnel and Ground Vibrations, *International Journal of Structural Stability and Dynamics*, 21(07), 2021, 2150101.
- [30] dos Santos, D.P., Gidrão, G.D., Carrazedo, R. A Simplified Numerical Model for the Assessment of Vibration in Subway Lines with Experimental Validation, *International Journal of Structural Stability and Dynamics*, 21(11), 2021, 2150156.
- [31] Fischer, S. Investigation of effect of water content on railway granular supplementary layers, *Naukovyi Visnyk Natsionalnoho Hirnychoho Universytetu*, 3, 2021, 64-68.
- [32] Juhasz, E., Fischer, S. Investigation of railroad ballast particle breakage, *Pollack Periodica*, 14(2), 2019, 3-14.
- [33] Kurhan, M., Kurhan, D. Railway track representation in mathematical model of vehicles movement, *Science and Transport Progress*, 6(72), 2017, 40-48.

ORCID iD

Dmytro Kurhan  <https://orcid.org/0000-0002-9448-5269>

Szabolcs Fischer  <https://orcid.org/0000-0001-7298-9960>



© 2022 Shahid Chamran University of Ahvaz, Ahvaz, Iran. This article is an open access article distributed under the terms and conditions of the Creative Commons Attribution-NonCommercial 4.0 International (CC BY-NC 4.0 license) (<http://creativecommons.org/licenses/by-nc/4.0/>).

How to cite this article: Kurhan D., Fischer S. Modeling of the Dynamic Rail Deflection using Elastic Wave Propagation, *J. Appl. Comput. Mech.*, 8(1), 2022, 379-387. <https://doi.org/10.22055/JACM.2021.38826.3290>

Publisher's Note Shahid Chamran University of Ahvaz remains neutral with regard to jurisdictional claims in published maps and institutional affiliations.

